JOURNAL OF MATERIALS SCIENCE 27 (1992) 4797–4804

Sintering behaviour of pyrophyllite mineral: effect of some alkali and alkaline-earth metal carbonates

S. S. AMRITPHALE, NAVIN CHANDRA, RAJENDRA KUMAR
Regional Research Laboratory (CSIR), Habib Ganj Naka, Hoshangabad Road, Bhopal 462 026, Madhya Pradesh, India

Pyrophyllite mineral was heat treated with alkali and alkaline-earth metal carbonates in equimolar ratios at 1000 °C for 2 h and the various phases formed in the sintered products were investigated using X-ray powder diffraction and infrared spectroscopy. The morphology of the products was studied using scanning electron microscopy. In each case formation of aluminosilicate phase of respective cation was observed, but the presence of mullite in sintered products was not detected.

1. Introduction

On heat treatment at sufficiently high temperatures, aluminosilicate minerals convert to a silica-rich vitreous phase and fibre-structured mullite. The formation of mullite in these minerals normally takes place at temperatures above 1000 °C [1, 2] but in the presence of small amounts of certain mineralizers, this temperature is lowered [3]. However, when the content of the mineralizers is high, the formation of new phases takes place in place of mullite. Carmen and Claudio observed the formation of $SrAl_2Si_2O_8$ and feldspar on reaction of kaolin with strontium carbonate in equimolar proportion in temperature range 900–1100 °C [4], and of hexacelsian and celsian on reaction of kaolin with equimolar ratio of barium carbonate in the temperature range 900–1100 °C [5].

Pyrophyllite, which also is an aluminosilicate mineral (ideal formula $Al_4Si_8O_{20}(OH)_4$), possesses a structure wherein an octahedral Al–O(OH) layer is sandwiched between two sheets of SiO_4 tetrahedra [6]. On heating it loses its hydroxyl water in the temperature range 550–900 °C forming dehydroxylate pyrophyllite [7] which is stable over a wide range of temperature [8–10]. Further heating destroys its structure and by topotactic reaction mullite and cristobalite start forming at a temperature of 1100 °C [8, 11]. The sintering behaviour studies carried out in the presence of small amounts (up to 2%) of added calcium, sodium, potassium and lithium carbonates showed the presence of mullite in the sintered products [12]. Similar to this observation, Sadukasov *et al.* [13] also detected mullite formation at 900 °C on sintering of pyrophyllite with up to 2% potassium oxide. However, no studies on the sintering behaviour of pyrophyllite with a high content of mineralizers have been reported in the literature. Because pyrophyllite possesses many significant properties and is used for a variety of applications after sintering at elevated temperatures, with or without additives [14–22], it was considered worthwhile to investigate its sintering behaviour in the presence of added alkali and alkaline-earth metal carbonates (in equimolar proportions) using X-ray powder diffraction, infrared spectroscopy and scanning electron microscopy. The results of these studies are presented in this paper.

2. Experimental procedure

The lithium, sodium, potassium, calcium and magnesium carbonates used in this study were of laboratory reagent grade.

Pyrophyllite mineral, collected from Khari mines of Tikamgarh district of Madhya Pradesh (chemical analysis: SiO_2 64.3%, Al_2O_3 23.9%, Fe_2O_3 2.1%, TiO_2 1%, MgO 0.8%, CaO 1.7%, K_2O 0.4%, Na_2O 0.1%, LOI 5.6%) was powdered (78% of the powder was in the particle size range 63–75 μm, and the balance 22%, was below 63 μm size). The powder was mixed mechanically with its respective reactant in equimolar proportion and heat treated at 1000 ± 5 °C for 2 h in an electrical muffle furnace. The resultant product was studied using a Philips X-ray difractrometer model 1710, with nickel-filtered CuK_α radiation. The identification of the phases formed was carried out by comparing the experimentally observed interplanar spacing (d values) and intensity of the peak with d values of the respective likely substances/phases given in the Mineral Powder Diffraction File Search Manual [23]. The infrared spectra were obtained using a Perkin–Elmer model 983 G in spectroscopic grade KBr in the wave number range 400–4000 cm^{-1}. The morphology of the sintered material was studied using a Jeol scanning electron microscope (Model-JEM-35-CF).

0022–2461

3. Results and discussion

3.1. X-ray powder diffraction studies

The X-ray powder diffraction (XRD) data for pyrophyllite mineral and samples obtained by its heat treatment in the presence of magnesium, calcium, potassium, sodium and lithium carbonates are given in Tables I–VI, respectively.

The *d* values obtained for Tikamgarh pyrophyllite sample (0.306, 0.459 and 0.443 nm) closely match the standard *d* values for the mineral (0.308, 0.458, 0.440 nm, respectively). These results confirm that in the sample the major phase is a double-layer monoclinic pyrophyllite with additional mineral phases of quartz and kaolinite (*d* values 0.334, 0.426, 0.182 nm and 0.149, 0.358, 0.414 nm, respectively) present in minor quantities as is evident from the relative intensities (cf. Table I).

The XRD results for the samples heat treated with magnesium carbonate (Table II) and calcium carbonate (Table III) show the presence of $Mg_3Al_2(SiO_4)_3$ and $CaAl_2Si_2O_8$, respectively, in addition to dehydroxylate pyrophyllite which is present as a major phase. The comparison of relative intensities of the phases formed with that of the dehydroxylate pyrophyllite shows that while $Mg_3Al_2(SiO_4)_3$ is present as a minor phase, (cf. Table II), $CaAl_2Si_2O_8$ is present as the next major phase.

In the case of samples sintered with potassium, sodium and lithium carbonates (cf. Tables IV–VI) the *d* values confirm that the phases formed are $KAlSiO_4$, $NaAlSiO_4$ (nepheline), $LiAl(SiO_3)_2$, respectively.

From the magnitude of the intensities of the respective phases formed, it is inferred that the effectiveness of the five additives studied is in the order: $Li_2CO_3 > Na_2CO_3 > K_2CO_3 > CaCO_3 > MgCO_3$, which follows the order of the strength of the bond between oxygen and the respective cation.

3.2. Infrared (IR) spectroscopy

To complement the X-ray results by assigning absorption frequencies corresponding to characteristic vibrations of different bonds in the molecules present in sintered products, the IR spectra were recorded. The IR spectra of pyrophyllite mineral alone (recorded for the sake of comparison) and samples heat treated with magnesium, calcium, potassium, sodium and lithium carbonates are shown in Figs 1–6, respectively. Similar

TABLE I X-ray powder diffraction analysis data for the pyrophyllite mineral

Experimental values for pyrophyllite mineral		Standard values					
		Pyrophyllite		Kaolinite		Quartz	
d(nm)	I/I_0	*d*(nm)	I/I_0	*d*(nm)	I/I_0	*d*(nm)	I/I_0
0.715 13	69						
0.499 13	77						
0.459 25	1978	0.458	50				
0.4437	364	0.440	20				
0.4226	248					0.426	40
0.4177	254	0.417	16				
0.4108	178			0.414	35		
0.3871	63			0.384	40		
0.3724	78			0.374	25		
0.3572	75			0.358	80		
0.351 14	107			Unidentified			
0.333 36	165					0.334	100
0.318 76	92			Unidentified			
0.306 22	3926	0.308	100				
0.298 76	160	0.297	2				
0.279 03	76			0.275	20		
0.256 80	222	0.259	6				
0.254 99	271	0.255	10				
0.253 12	342			0.253	35		
0.241 40	398	0.244	16				
0.229 79	186	0.231	6				
0.216 46	112	0.217	6				
0.214 92	137						
0.208 42	156	0.209	6				
0.205 83	167	0.207	6				
0.189 10	86	0.1895	2				
0.183 85	345	0.1848	6			0.182	20
0.169 10	88	0.1692	6				
0.166 74	77						
0.164 60	166	0.1650	10				
0.162 95	170	0.15					
0.153 30	71	0.1542	6				
0.149 28	193	0.1492	10	0.149	100		
0.138 41	221	0.1388	10				
0.136 95	183	0.1373	10				

TABLE II X-ray powder diffraction analysis data for the sintered pyrophyllite–magnesium carbonate system

Experimental values for sintered sample		Standard values			
		Dehydroxylated pyrophyllite		$Mg_3Al_2(SiO_4)_3$	
d(nm)	I/I_0	d(nm)	I/I_0	d(nm)	I/I_0
0.536 32	108				
0.498 82	111	0.499	2		
0.462 93	258	0.459	50		
0.447 11	154	0.443	20		
0.439 77	183				
0.416 09	124	0.417	16		
0.405 41	164	0.410	5		
0.385 79	138	0.387	2		
0.376 58	130				
0.370 35	119	0.372	2		
0.349 38	141				
0.340 65	194				
0.337 02	218				
0.333 84	250	0.333	4		
0.321 16	107	0.318	2		
0.309 45	695	0.306	100		
0.296 24	90	0.298	2		
0.290 91	93				
0.283 98	114				
0.275 25	74	0.279	2		
0.268 16	83				
0.257 97	77	0.256		0.259	100
0.253 33	100	0.254			
0.244 99	112				
0.242 25	152	0.241			
0.235 55	54				
0.220 23	83				
0.211 89	95				
0.209 74	149	0.216		0.210	100
0.200 61	102	0.208			
0.186 17	58	0.205			
0.172 37	49	0.189			
0.165 99	80	0.169		0.162	90
0.154 89	79	0.166			
0.152 23	71	0.153			
0.144 02	50				
0.142 37	102				

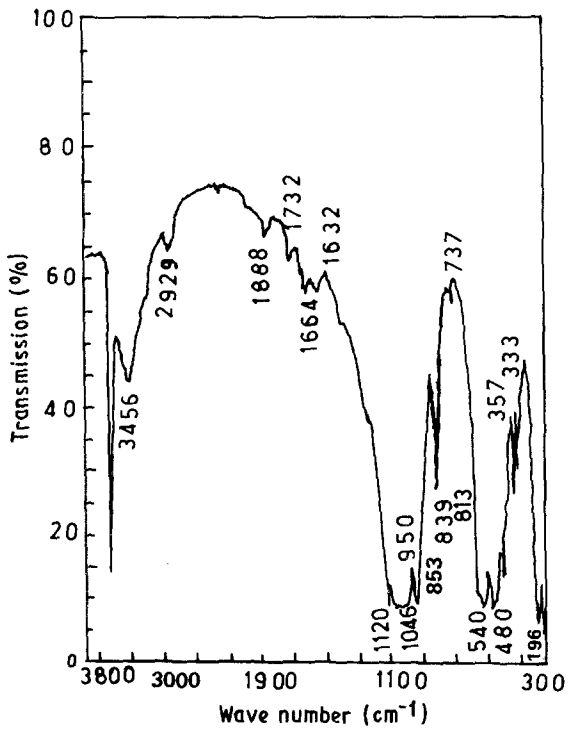

Figure 1 Infrared spectra of the pyrophyllite mineral.

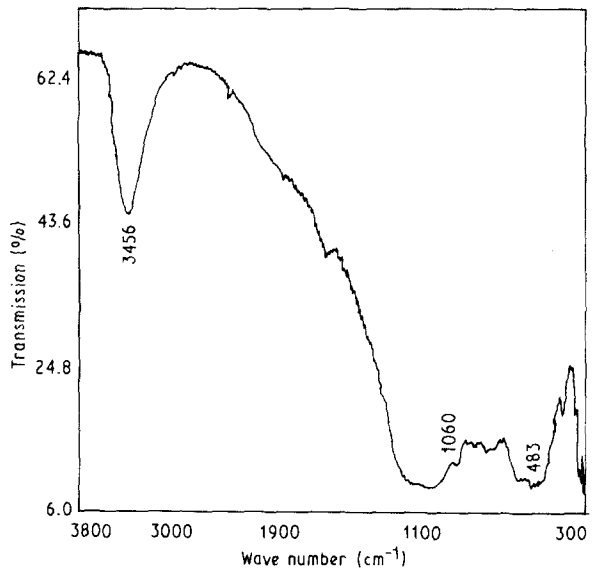

Figure 2 Infrared spectra of the sintered pyrophyllite–magnesium carbonate system.

TABLE III X-ray powder diffraction analysis data for the sintered pyrophyllite–calcium carbonate system

Experimental values for sintered sample		Standard values			
		Dehydroxylated pyrophyllite		$CaAl_2Si_2O_8$	
d(nm)	I/I_0	d(nm)	I/I_0	d(nm)	I/I_0
0.73599	49				
0.53959	48				
0.49962	68	0.499	2		
0.46269	111	0.459	50		
0.44517	246	0.443	20		
0.43937	180				
0.42680	110	0.4226			
0.40034	71	0.4108			
0.38092	250	0.387		0.380	100
0.37099	338	0.372			
0.36139	71	0.357			
0.34896	157	0.351			
0.33988	87				
0.33341	223	0.333			
0.32860	162				
0.32122	160				
0.31770	144	0.318			
0.30911	313	0.306	100		
0.30343	82				
0.30080	86				
0.29610	94	0.298	2		
0.28525	217			0.284	90
0.28227	256				
0.27927	110	0.279			
0.26968	55				
0.26487	39				
0.26121	58				
0.25747	154	0.2568	6	0.256	80
0.25477	101	0.254	10		
0.25031	79	0.253			
0.24170	76	0.241	16		
0.22713	57	0.229	6		
0.21646	63	0.216	6		
0.21148	65	0.214	6		
0.26296	59	0.205	6		
0.19847	55	0.189	2		
0.19690	58				
0.18687	68				
0.18284	54	0.183	6		
0.17440	62				
0.15113	47	0.153	6		
0.15073	63				

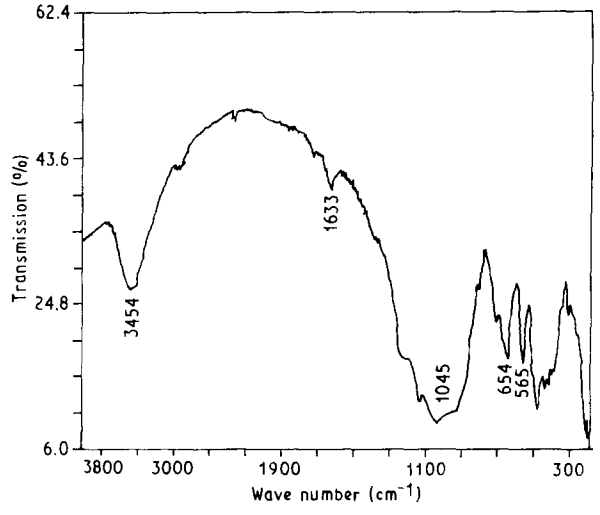

Figure 3 Infrared spectra of the sintered pyrophyllite–calcium carbonate system.

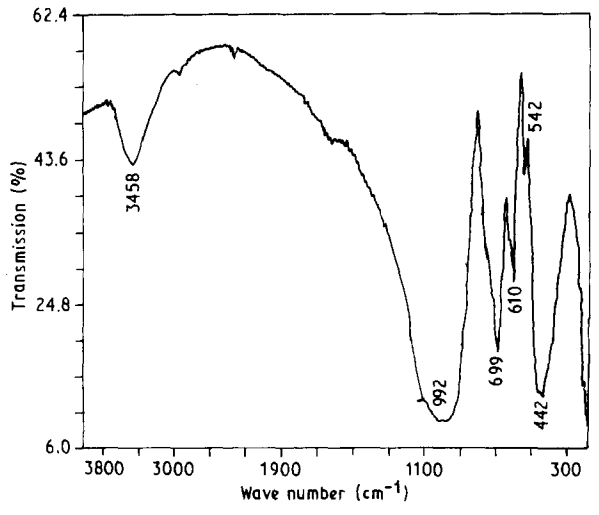

Figure 4 Infrared spectra of the sintered pyrophyllite–potassium carbonate system.

TABLE IV X-ray powder diffraction analysis data for the sintered pyrophyllite–potassium carbonate system

Experimental values for sintered sample		Standard values $KAlSiO_4$	
d(nm)	I/I_0	d(nm)	I/I_0
0.57308	64		
0.54698	122		
0.53436	362		
0.47007	80		
0.44904	83	0.449	8
0.42639	167	0.426	15
0.38541	70	0.390	10
0.35813	78		
0.35428	161		
0.34901	115	0.350	10
0.34167	574		
0.32521	874		
0.31587	78		
0.30973	858	0.309	100
0.30302	61	0.302	12
0.29099	230		
0.28286	267		
0.27926	238		
0.26726	97		
0.26303	100		
0.25997	262	0.2599	30
0.23597	148		
0.22984	58		
0.22233	87	0.224	4
0.21367	163	0.213	25
0.20667	52		
0.20485	58		
0.19134	41		
0.18646	49		
0.17240	73		
0.16646	95		
0.15846	71		
0.15308	52		
0.15068	54		

TABLE V X-ray powder diffraction analysis data for the sintered pyrophyllite–sodium carbonate system

Experimental values for sintered sample		Standard values: $NaAlSiO_4$ (nepheline)	
d(nm)	I/I_0	d(nm)	I/I_0
0.85977	99		
0.49713	168		
0.43059	366	0.430	10
0.41654	786	0.419	45
0.38290	1084	0.383	65
0.37519	118	0.377	10
0.34912	90		
0.32597	750	0.326	55
0.30347	188	0.304	10
0.29984	1125	0.300	100
0.28764	560	0.288	45
0.25700	286	0.2568	25
0.24905	179	0.249	16
0.23949	154	0.239	16
0.23381	490	0.233	40
0.23015	247	0.2301	20
0.21587	76	0.216	6
0.21163	107	0.2118	10
0.20867	181	0.208	16
0.20283	71	0.202	2
0.19797	68	0.198	2
0.19275	115	0.1927	10
0.17906	87	0.1787	10
0.16916	94	0.1688	6
0.16332	67	0.1633	6
0.16148	100	0.1612	10
0.15981	103	0.159	10
0.15592	192	0.155	25
0.15228	66	0.152	6
0.14681	70	0.1465	6
0.14277	79	0.1425	10
0.13847	158	0.1384	20
0.13718	66	0.1367	6

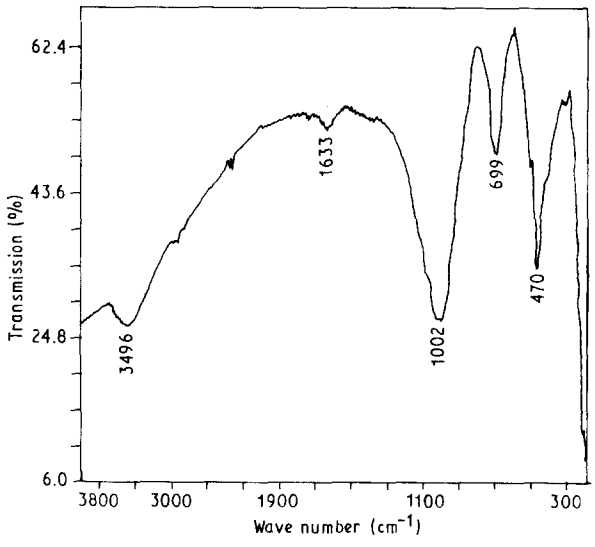

Figure 5 Infrared spectra of the sintered pyrophyllite–sodium carbonate system.

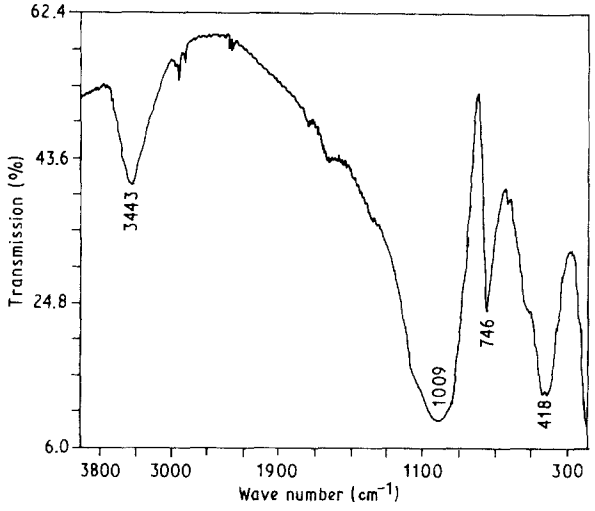

Figure 6 Infrared spectra of the sintered pyrophyllite–lithium carbonate system.

to the observation of Khandal and Gangopadhyay [24] in the IR spectra of clays, the peaks observed by us in the IR spectra of pyrophyllite (Fig. 7) at 3673 cm^{-1} may be assigned to the O–H vibration of the Al–OH linkage, while the peak at wave number 3461 cm^{-1} may be due to the O–H stretching of the surface water, and the peak at 1633 cm^{-1} may be assigned to bending of the O–H surface group [24]. The peak at 1121 cm^{-1} is assigned to Al–OH vibration following Miller [25]. The peak at 1045 cm^{-1}

TABLE VI X-ray powder diffraction analysis data for the sintered pyrophyllite–lithium carbonate system

Experimental values for sintered sample		Standard values: $LiAl(SiO_3)_2$	
d(nm)	I/I_0	d(nm)	I/I_0
0.622 34	122		
0.550 27	83		
0.536 82	227		
0.449 61	61		
0.453 24	786	0.452	10
0.386 34	34		
0.348 83	7183	0.348	100
0.342 82	376		
0.326 15	518		
0.291 59	142		
0.283 55	146		
0.280 71	103		
0.261 89	286		
0.248 36	42		
0.236 51	83		
0.234 00	109		
0.226 82	251		
0.212 78	53		
0.209 51	212		
0.189 17	928	0.189	2
0.174 61	75		
0.171 40	50		
0.163 71	402		
0.151 47	66		
0.145 39	185		
0.142 21	277		

corresponds to an Si–O linkage, characteristic of aluminosilicates [26], at 949 cm^{-1} to Al–(OH) and Si–O linkages [16], and peaks in the range 853–813 cm^{-1} and at 737 cm^{-1} show the presence of quartz and kaolinite [27, 28].

The peak at wave number 1120 cm^{-1} representing Al–O linkage, and those due to the presence of quartz observed in the IR spectra of the pyrophyllite sample, are found to disappear in the case of all six sintered samples. However, the peaks in the viscinity of wave numbers 3461 and 1633 cm^{-1} corresponding to the adsorbed surface water are still present as the sample was cooled in an open atmosphere after heat treatment. In addition to these peaks, in the case of heat-treated samples, new peaks appear [29] at wave numbers 1060 cm^{-1} corresponding to Mg–O linkages in $Mg_3Al_2(SiO_4)_3$ (Fig. 2), at 1045 cm^{-1} representing Ca–O linkages in $CaAl_2Si_2O_8$ (Fig. 3), at 992 cm^{-1} showing K–O linkages in $KAlSiO_4$ (Fig. 4), at 1002 cm^{-1} showing Na–O linkages in $NaAlSiO_4$ (Fig. 5) and at 1009 cm^{-1} corresponding to Li–O linkages in $LiAl(SiO_3)_2$ (Fig. 5).

3.3. Scanning electron microscopic studies

The scanning electron micrographs of heat-treated pyrophyllite mineral and samples sintered with magnesium, calcium, lithium, potassium and sodium carbonates are shown in Figs 7–12, respectively. Fig. 7 shows that the dehydroxylated pyrophyllite is flaky in nature. On sintering with magnesium carbonate, the flakiness is reduced and formation of crystals is seen

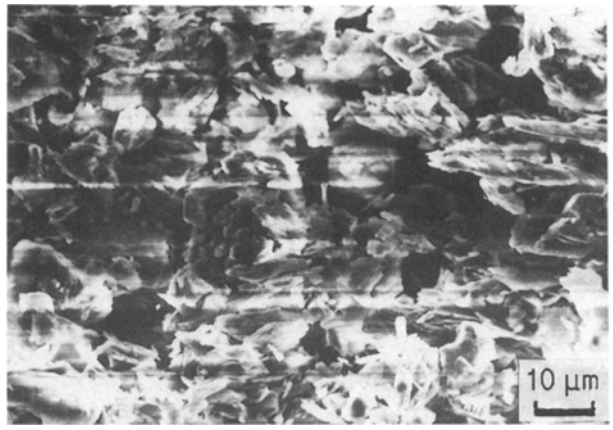

Figure 7 Scanning electron micrograph of dehydroxylate pyrophyllite.

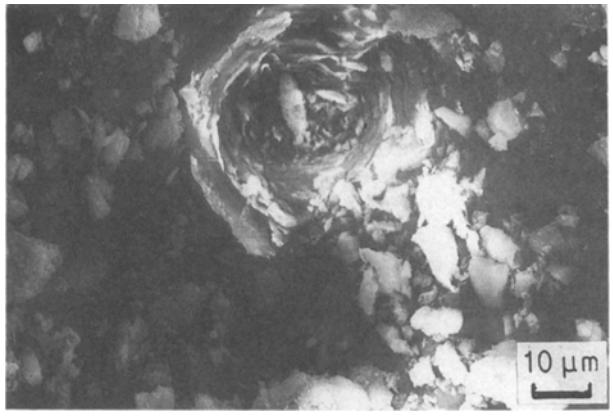

Figure 8 Scanning electron micrograph of the sintered pyrophyllite–magnesium carbonate system.

Figure 9 Scanning electron micrograph of the sintered pyrophyllite–calcium carbonate system.

(Fig. 8). The effect is further enhanced in the case of calcium carbonate (Fig. 9). In the case of heat treatment with alkali metal carbonates, the X-ray results have shown the predominant presence of new crystalline phases of aluminium silicates of alkali metal ions, which are clearly seen in their scanning electron micrographs. The crystals are smaller in size in the case of lithium carbonate (Fig. 10). In potassium carbonate, the crystals are larger (Fig. 11) compared to

Figure 10 Scanning electron micrograph of the sintered pyrophyllite–lithium carbonate system.

Figure 11 Scanning electron micrograph of the sintered pyrophyllite–potassium carbonate system.

Figure 12 Scanning electron micrograph of the sintered pyrophyllite–sodium carbonate system.

those observed with lithium carbonate. The crystals obtained with sodium carbonate are substantially larger in size (Fig. 12).

The mullite formation in pyrophyllite mineral takes place at temperatures above 1100 °C. The presence of small amounts of certain salts, called mineralizers, induces the catalytic mullite formation at a lower temperature [3, 12, 18]. However, if the content of the mineralizers is high, as in the case of the present study, the formation of mullite is not detected and instead, new phases of aluminosilicates of the respective cations are formed, as seen from the X-ray results. A similar observation has been reported by Carmen and Claudio [4, 5]. It is possible that even in low concentrations, the mineralizer reacts with the mineral to form the "new phases" but, owing to their low concentration, their presence is not detected. However, in the case of a high concentration of mineralizer, the silica is utilized in the formation of aluminosilicate phase of the respective cation and thus the formation of mullite is prevented.

4. Conclusion

The sintering of pyrophyllite with the carbonates of magnesium/calcium/potassium/sodium/lithium in equimolar ratios under the experimental conditions used, has been found to give rise to the formation of magnesium aluminium silicate ($Mg_3Al_2(SiO_4)_3$), calcium aluminium silicate ($CaAl_2Si_2O_8$), potassium aluminium silicate ($KAlSiO_4$), sodium aluminium silicate (nepheline, $NaAlSiO_4$) and lithium aluminium silicate ($LiAl(SiO_3)_2$), respectively. The formation of mullite, which takes place when pyrophyllite is sintered with small quantities of the above compounds, has not been detected in the present study. It is therefore inferred that the silica content of the mineral is effectively utilized by the cation for the formation of the above phases and thus prevents the formation of mullite. The ease of formation of these new phases, as indicated from the relative intensities in the XRD data, is found to be in the following order: $LiAl(SiO_3)_2 > NaAlSiO_4 > KAlSiO_4 > CaAl_2Si_2O_8 > Mg_3Al_2(SiO_4)_3$.

Acknowledgements

The authors thank the Director, R. R. L., Bhopal for his kind permission to publish this paper and Drs A. K. Jha and S. Das for their help in SEM and X-ray powder diffraction work.

References

1. G. CELOTTI and L. MORETTINI, *J. Mater. Sci.* **19** (1983) 838.
2. D. S. PERERA and G. ALLOTT, *J. Mater. Sci. Lett.* **4** (1985) 1270.
3. G. N. MASLENNIKOVA and T. I. KONESHOVA, *Steklo i Keramika* **4** (1987) 13.
4. G. M. CARMEN and G. CLAUDIO, *Trans. Br. Ceram. Soc.* **83** (1984) 200.
5. *Idem., ibid.* **83** (1984) 150.
6. J. H. LEE and S. GUGGENHEIM, *Amer. Mineral.* **66** (1981) 350.
7. R. WARDLE and G. W. BRINDLEY, *ibid.* **57** (1972) 732.
8. L. HELLER, *Amer. Mineral.* **47** (1962) 156.
9. K. J. D. MACKENZIE, I. W. M. BROWN, R. H. MEINHOLD and M. E. BOWDEN, *J. Amer. Ceram. Soc.* **68** (1985) 266.
10. J. S. PEDRO and L. P. JOSE, *J. Mater. Sci.* **24** (1989) 3774.
11. W. F. BRADLEY and R. E. GRIM, *Amer. Mineral.* **36** (1981) 350.
12. S. S. AMRITPHALE and M. PATEL, *J. X-ray Spectrom.* **17**(5) (1988) 181.

13. A. S. SADUKASOV, Kh. Zh. USIPBEKOVA and F. I. ZEL, *Tr. Khim. Met. Inst. Akad. Nauk KAL SSSR* **15** (1970) 168.
14. T. KANABARA, T. YAMAMOTO, H. IKAWA, T. TAGAWA and H. IMAI, *J. Mater. Sci.* **24** (1989) 1552.
15. S. S. AMRITPHALE, M. MAHESHWARI and M. PATEL, *J. Sci. Res.* **45** (1986) 66.
16. S. S. AMRITPHALE and M. PATEL, *J. Silicate Ind.* **3–4** (1987) 31.
17. S. S. AMRITPHALE, NAVIN CHANDRA and R. KUMAR, presented in "Seminar on Future Trends and Problems in Chemical Engineering Research and Industry", Institution of Engineers, Bhopal, 1988.
18. S. S. AMRITPHALE, C. B. RAJU and R. KUMAR, in "Proceedings of the Seminar on the Development of Mineral Resources of Madhya Pradesh", edited by Rajendra Kumar (Regional Research Laboratory, Bhopal, 1987) p. 183.
19. S. S. AMRITPHALE and M. PATEL, *J. Silicate Ind.* **5–6** (1990) 169.
20. K. C. RIEGER, *Amer. Ceram. Soc. Bull.* **69** (1990) 874.
21. J. MUKERJEE and S. BANDYOPADHYAY, *Ind. J. Tech.* **23** (1985) 227.
22. V. G. MALOGOLOVETS and A. V. GERASIMOVICH, *Sverkhtverd. Mater.* **1** (1988) 7.
23. "Mineral Powder Diffraction File Search Manual", (JCPDS, International, Centre for Diffraction Data, Swarthmore, USA, 1980).
24. R. K. KHANDAL and P. K. GANGOPADHYAY, *Ind. Ceram.* **28**(9) (1985) 195.
25. J. G. MILLER, *J. Phys. Chem.* **65** (1961) 800.
26. S. RAMAN and T. K. DAN, *Ind. Ceram.* **29**(2) (1986) 25.
27. J. GANGULI and B. K. BANERJEE, *ibid.* **27**(9) (1984) 173.
28. K. RAMASWAMY and M. KAMALAKKAN, *Ind. J. Pure Appl. Phys.* **25C** (1987) 284.
29. S. S. AMRITPHALE, PhD thesis, Barkatullah University, Bhopal (1990).

Received 8 May
and accepted 12 September 1991